Interlinked Fast and Slow Positive Feedback Loops Drive Reliable Cell Decisions

Onn Brandman, *et al.*

Science **310**, 496 (2005);
DOI: 10.1126/science.1113834

mounting a substantial TSE interference effect. No immune system cells were necessary for this protection, and stable interfering infections were reproducibly achieved without cloning. Interference did not depend on the presence or absence of abnormal PrP. Only persistent infection protected target cells from superinfection. Additionally, only particular agent-strain combinations showed positive interference, and these could not be predicted from cellular PrPres amounts or banding patterns. Moreover, despite continuous replication in cells with PrPres band patterns very different from those found in brain tissue, SY and FU CJD agents each breed true when reinoculated into mice, as does rodent-passaged scrapie reinoculated in sheep (*10*). The stability of the BSE agent also contrasts with the many different PrPres patterns seen in various affected species. Together, these results are not compatible with the common assumption that TSE strains are encoded by some unresolved type of PrPres folding (*16*, *17*). Indeed, there is still no conclusive evidence that any recombinant or amplified form of abnormal PrP can infect normal animals directly, reproduce meaningful levels of infectivity, or encode all the strain differences observed in mice infected with scrapie, CJD, and BSE agents.

Unlike heterogeneous aggregates of pathological PrP, infectious TSE particles have a discrete viral size of ~25 nm and 10^7 daltons (as assessed by field flow fractionation and high-pressure liquid chromatography, respectively) (*18*), and releasing their tightly bound nucleic acids destroys infectivity (*19*). Thus, some TSE agents such as SY may produce defective interfering particles, as found in many persistent viral as well as noncoding human viroid infections (*20*, *21*). Unlike pathologic host PrP, TSE agents can also provoke innate cellular defenses, including intracellular and diffusible factors that are not restricted to immune system cells (*7*, *8*), and such factors are likely to be involved in interference. Small interfering RNAs with extensive secondary structure may also be evoked by TSE agents, and these can provide even greater strain specificity (*22*). Notably, several small RNAs with extensive secondary structure have been identified in TSE-infected but not in normal brain tissue (*23*), and such motifs deserve further study in TSE culture models.

Cocultures were more efficient than mouse bioassays and can be useful for rapid assessment of agent purification and recovery (*24*). Additionally, they may provide a sensitive test for cells that are infected but show no PrPres (such as white blood cells), and they may be useful for evaluating a wide range of evolving TSE agents that have become important epidemiologically, such as those that cause BSE and chronic wasting disease (CWD). The resistance of cells infected with a prototypic sporadic CJD agent (SY) to two scrapie strains supports the suggestion that a commensal but rarely pathogenic TSE agent may help protect people against infection by sheep TSE strains in nature (*4*), and may explain why so few people have developed BSE-linked CJD (*25*). The clustering of sporadic CJD cases is also consistent with an environmental agent of low virulence (*26*).

References and Notes

1. L. Manuelidis, W. Fritch, Y. G. Xi, *Science* **277**, 94 (1997).
2. L. Manuelidis, *Proc. Natl. Acad. Sci. U.S.A.* **95**, 2520 (1998).
3. L. Manuelidis, Z. Y. Lu, *Neurosci. Lett.* **293**, 163 (2000).
4. L. Manuelidis, Z. Y. Lu, *Proc. Natl. Acad. Sci. U.S.A.* **100**, 5360 (2003).
5. A. Dickinson, H. Fraser, V. Meikle, G. Outram, *Nature New Biol.* **237**, 244 (1972).
6. C. Baker, L. Manuelidis, *Proc. Natl. Acad. Sci. U.S.A.* **100**, 675 (2003).
7. C. Baker, Z. Lu, L. Manuelidis, *J. Neurovirol.* **10**, 1 (2004).
8. Z. Lu, C. Baker, L. Manuelidis, *J. Cell. Biochem.* **93**, 644 (2004).
9. N. Nishida *et al.*, *J. Virol.* **74**, 320 (2000).
10. A. Arjona, L. Simarro, F. Islinger, N. Nishida, L. Manuelidis, *Proc. Natl. Acad. Sci. U.S.A.* **101**, 8768 (2004).
11. See supporting data on *Science* Online.
12. C. Lasmezas *et al.*, *Science* **275**, 402 (1997).
13. Y. G. Xi, A. Ingrosso, A. Ladogana, C. Masullo, M. Pocchiari, *Nature* **356**, 598 (1992).
14. A. Hill *et al.*, *Brain* **126**, 1333 (2003).
15. L. Manuelidis *et al.*, *J. Virol.* **74**, 8614 (2000).
16. S. Prusiner, *Proc. Natl. Acad. Sci. U.S.A.* **95**, 13363 (1998).
17. G. S. Jackson, J. Collinge, *Mol. Pathol.* **54**, 393 (2001).
18. T. Sklaviadis, R. Dreyer, L. Manuelidis, *Virus Res.* **3**, 241 (1992).
19. L. Manuelidis, T. Sklaviadis, A. Akowitz, W. Fritch, *Proc. Natl. Acad. Sci. U.S.A.* **92**, 5124 (1995).
20. A. Barrett, *Curr. Top. Microbiol. Immunol.* **128**, 55 (1986).
21. J. Wu *et al.*, *World J. Gastroenterol.* **11**, 1658 (2005).
22. P. M. Waterhouse, M. B. Wang, T. Lough, *Nature* **411**, 834 (2001).
23. L. Manuelidis, in *Transmissible Subacute Spongiform Encephalopathies: Prion Diseases*, L. Court, B. Dodet, Eds. (Elsevier, Paris, 1966), pp. 375–387.
24. L. Manuelidis *et al.*, unpublished data.
25. L. Linsell *et al.*, *Neurology* **63**, 2077 (2004).
26. P. Smith, S. Cousens, J. d'Huillard Aignaux, H. Ward, R. Will, *Curr. Top. Microbiol. Immunol.* **284**, 161 (2004).

27. Supported by NIH grant NS12674, U.S. Department of Defense grant DAMD-17-03-1-0360, and a grant from the Ministry of Health, Labor and Welfare, Japan.

Supporting Online Material
www.sciencemag.org/cgi/content/full/310/5747/493/DC1
Materials and Methods

29 July 2005; accepted 21 September 2005
10.1126/science.1118155

Interlinked Fast and Slow Positive Feedback Loops Drive Reliable Cell Decisions

Onn Brandman,[1,2]* James E. Ferrell Jr.,[1] Rong Li,[2,3,4] Tobias Meyer[1,2]

Positive feedback is a ubiquitous signal transduction motif that allows systems to convert graded inputs into decisive, all-or-none outputs. Here we investigate why the positive feedback switches that regulate polarization of budding yeast, calcium signaling, *Xenopus* oocyte maturation, and various other processes use multiple interlinked loops rather than single positive feedback loops. Mathematical simulations revealed that linking fast and slow positive feedback loops creates a "dual-time" switch that is both rapidly inducible and resistant to noise in the upstream signaling system.

Studies in many biological systems have identified positive feedback as the key regulatory motif in the creation of switches with all-or-none "digital" output characteristics (*1*). Although a single positive feedback loop (*A* activates *B* and *B* activates *A*) or the equivalent double-negative feedback loop (*A* inhibits *B* and *B* inhibits *A*) can, under the proper circumstances, generate a bistable all-or-none switch (*1*–*5*), it is intriguing that many biological systems have not only a single but multiple positive feedback loops (Table 1). Three examples of positive feedback systems are shown in more detail in Fig. 1.

[1]Department of Molecular Pharmacology, Stanford University School of Medicine, Stanford, CA, 94305, USA. [2]Physiology Course 2004, Marine Biological Laboratory, Woods Hole, MA 02543, USA. [3]Department of Cell Biology, Harvard Medical School, Boston, MA 02115, USA. [4]The Stowers Institute for Medical Research, Kansas City, MO 64110, USA.

*To whom correspondence should be addressed. E-mail: onn@stanford.edu

Polarization in budding yeast depends on two positive feedback loops, a rapid loop involving activity cycling of the small guanosine triphosphatase Cdc42 and a slower loop that may involve actin-mediated transport of Cdc42 (Fig. 1A) (*6*). In many cell types, the induction of prolonged Ca^{2+} signals involves initial rapid positive feedback loops centered on Ca^{2+} release mediated by inositol 1,4,5-trisphosphate (IP3) combined with a much slower loop that induces Ca^{2+} influx mediated by the depletion of Ca^{2+} stores (*7*, *8*) (Fig. 1B). *Xenopus* oocytes respond to maturation-inducing stimuli by activating a rapid phosphorylation/dephosphorylation–mediated positive feedback loop (between Cdc2, Myt1, and Cdc25) and a slower translational positive feedback loop [between Cdc2 and the the mitogen-activated protein kinase (MAPK or ERK) cascade, which includes Mos, MEK (MAPK kinase), and p42] (Fig. 1C).

The presence of multiple interlinked positive loops raises the question of the performance

Table 1. Examples of interlinked positive feedback loops in biological regulation.

System	Positive feedback loops	References
Mitotic trigger	Cdc2 → Cdc25 → Cdc2 Cdc2 -| Wee1 -| Cdc2 Cdc2 -| Myt1 -| Cdc2	(*12*, *13*)
p53 regulation	p53 → PTEN -| Akt → Mdm-2 -| p53 p53 → p21 -| CDK2 -| Rb -|Mdm-2 -| p53	(*14*)
Xenopus oocyte maturation	Cdc2 → Mos → Cdc2 Cdc2 → Cdc25 → Cdc2 Cdc2 → Myt1 → Cdc2	(*11*)
Budding yeast traversal of START	Cdc28 → Cln transcription → Cdc28 Cdc28 -| Sic1 -| Cdc28	(*15*)
Budding yeast polarization	Cdc42 → Cdc24 → Cdc42 Cdc42 → actin → Cdc42	(*6*, *16*, *17*)
Eukaryotic chemotaxis	PIP_3 → Rac/Cdc42 → PIP_3 PIP_3 → Rac/Cdc42 → actin → PIP_3	(*18*)
Muscle cell fate specification	MyoD → MyoD Myogenin → myogenin MyoD → CDO → MyoD MyoD → Akt2 → MyoD	(*19*–*21*)
B cell fate specification	IL-7 → EBF → IL-7 EBF -| Notch-1 -|E2A → EBF → Pax-5 -| Notch-1 -| E2A→ EBF	(*22*, *23*)
Notch/delta signaling	Notch (cell A) -| Delta (cell A) -| Notch (cell A) Notch (cell A) -| Delta (cell A) → Notch (cell B) -| Delta (cell B) → Notch (cell A)	(*24*)
EGF receptor signaling	EGFR -| PTP -| EGFR Sos → Ras → Sos ERK2 → arachidonic acid → ERK2 EGFR → sheddases → EGFR	(*25*–*28*)
S. cerevisiae galactose regulation	Gal2 → galactose -| Gal80 -| Gal2 Gal3 -| Gal80 -| Gal3	(*29*)
Blood clotting	thrombin → Xa:Va → thrombin XIIa → XIIa IXa:VIIIa → Xa → IXa:VIIIa	(*30*)
Platelet activation	activation → ADP secretion → activation activation → 5-HT secretion → activation activation → TxA_2 secretion → activation activation → aggregation → activation	(*31*)
Ca^{2+} spikes/oscillations	Ca^{2+}_{cyt} → PLC → IP_3 → Ca^{2+}_{cyt} Ca^{2+}_{cyt} → IP_3R → Ca^{2+}_{cyt} Ca^{2+}_{cyt} → IP_3R -| Ca^{2+}_{ER} -| SOC → Ca^{2+}_{cyt}	(*7*, *8*)

ADP, adenosine 5′-diphosphate; CDK, cyclin-dependent kinase; cyt, cytochrome; CDO, a component of a cell surface receptor; EGFR, epidermal growth factor receptor; ER, endoplasmic reticulum; 5-HT, serotonin (5-hydroxytryptamine); IL-7, interleukin-7; IP_3R, inositol 1,4,5-trisphosphate receptor; PIP_3, phosphatidylinositol 3,4,5-trisphosphate; PLC, phospholipase C; PTEN, phosphatase and tensin homolog deleted on chromosome 10; PTP, protein tyrosine phosphatase; *S. cerevisiae*, *Saccharomyces cerevisiae*; TxA_2, thromboxane A_2.

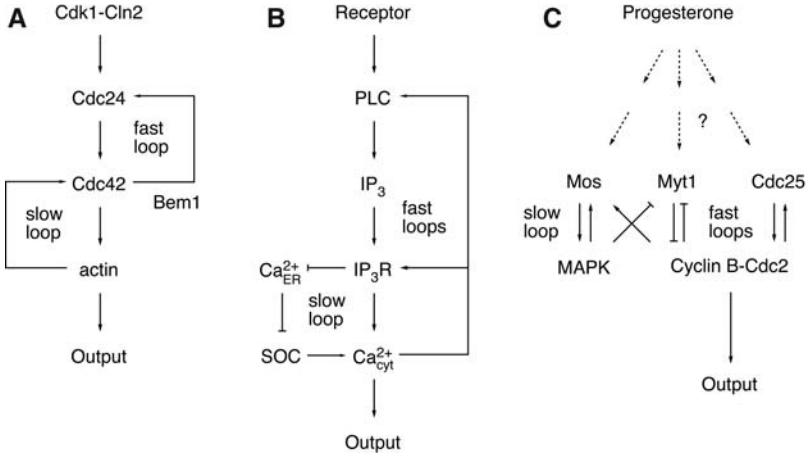

Fig. 1. Schematic views of positive feedback loops in three systems. (**A**) Establishment of polarity in budding yeast. (**B**) Mammalian calcium signal transduction. (**C**) *Xenopus* oocyte maturation.

advantage of the multiple-loop design. One clue is provided by recent studies of budding yeast polarization. When the slow positive feedback loop is selectively compromised by treatment with the actin-depolymerizing agent latrunculin, the result is rapid but unstable cell polarization (*6*). In contrast, cells lacking a functional fast loop (by deletion of Bem1) form stable poles, but with reduced speed (*6*). These experimental observations led us to hypothesize that the slow positive feedback loop is crucial for the stability of the polarized "on" state, whereas the fast loop is critical for the speed of the transition between the unpolarized "off" state and polarized on state.

To test this hypothesis computationally, we created models of positive feedback switches containing either a single positive feedback loop (Fig. 2A) or two interlinked loops (Fig. 2B). For the single-loop switch, we assumed either fast or slow kinetics for the activation and inactivation of loop component *A*. For the dual-loop switch, we assumed either fast kinetics for both the *A* and *B* loops, slow kinetics for both loops, or fast kinetics for the *A* loop and slow for the *B* loop (*9*).

Each model switch responded to a noise-free stimulus (Fig. 2, C to G, left) and a noisy stimulus (Fig. 2, C to G, right) as shown. As expected, the single-slow-loop switch turned on and off slowly and filtered out noise (Fig. 2C). Adding a second slow loop produced a higher basal activity in the off state, a quicker switch from off to on, and a slower switch from on to off (Fig. 2D). The behavior of the two-slow-loop switch was exactly equivalent to that of a single-loop switch in which the concentration of *B* was doubled. Thus, adding a second loop with identical kinetic constants provides a back-up in the event of gene deletion, but does not otherwise alter the behavior of the system beyond what could be achieved with a single loop.

The single-fast-loop switch turned on and off rapidly and was highly susceptible to noise in both the off and on states (Fig. 2E), and adding a second fast loop quickened the transition from off to on and delayed the transition from on to off (Fig. 2F). Thus, the fast-loop switch achieved more rapid responses, but at the cost of increased noise.

In contrast, the system in which a slow and a fast positive feedback loop are linked together introduces marked advantages over single-loop systems, as well as dual-loop systems with the same time constant. In this "dual-time" switch, the output turned on rapidly, as a consequence of the kinetic properties of the fast loop, and turned off slowly as a consequence of the kinetics of the slow loop (Fig. 2G). This allows for independent tuning of the activation and deactivation times. More important, although the dual-time switch exhibited high noise sensitivity when in the off state, as a result of the rapid responses of its fast loop, it became resistant to noise once it settled in its on state as a result of the properties of its slow loop. Thus,

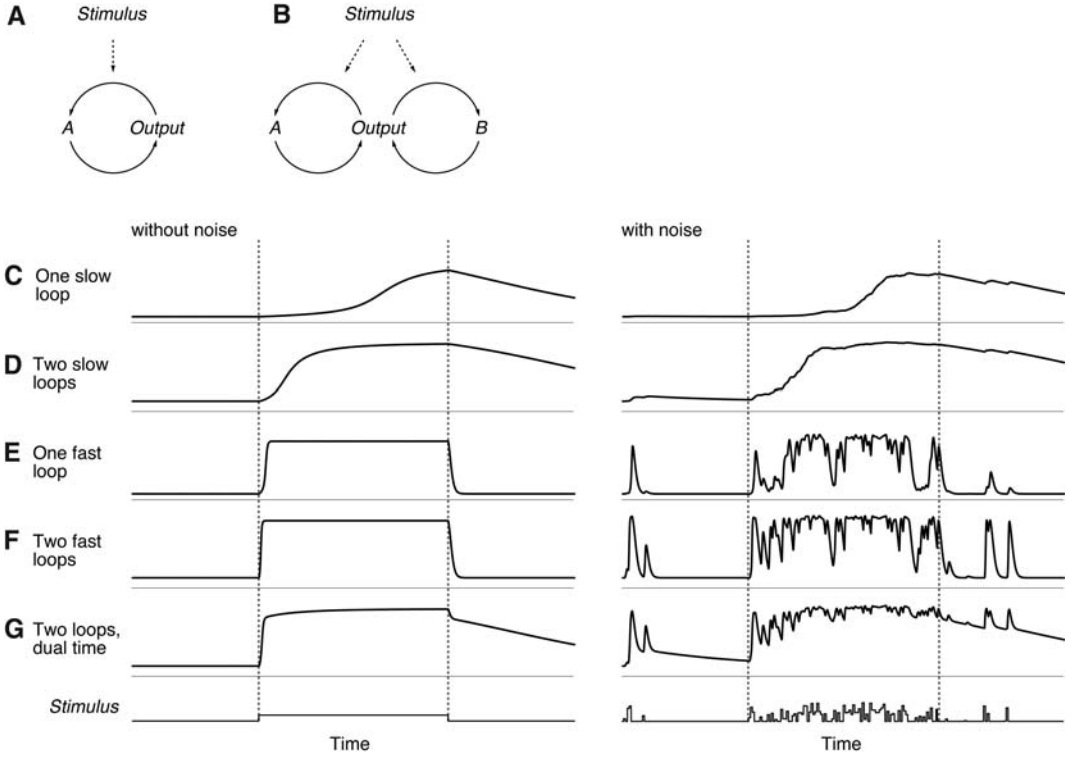

Fig. 2. Calculated responses of single and dual positive feedback loop switches to stimuli. (**A**) A one-loop switch. (**B**) A two-loop switch. (**C** to **G**) Feedback loop output (*y* axis) as a function of time (*x* axis) for single-loop and two-loop switches. (**C**) One slow loop. (**D**) Two slow loops. (**E**) One fast loop. (**F**) Two fast loops. (**G**) One slow loop and one fast loop. The curves on the left assume a noise-free stimulus; the curves on the right assume a noisy stimulus.

the dual-time switch provides the ability to transit rapidly from the off state to the on state together with robust stability of the on state (*10*).

These computational studies help understand the yeast phenotypes described above and provide a rationale for the existence of dual-time positive feedback systems in Ca^{2+} signaling, oocyte maturation, and other biological systems. In the case of Ca^{2+} signaling, the dual-time system enables rapid Ca^{2+} responses from IP3-induced Ca^{2+} release, while also enabling long-term robust Ca^{2+} signals once the store-operated Ca^{2+} influx is triggered. Although weak stimuli or noise have been shown to trigger IP3-mediated Ca^{2+} spikes, more persistent stimuli are needed to induce Ca^{2+} influx and prolonged Ca^{2+} responses (*7*). These long-term Ca^{2+} signals are required for T-cell activation and differentiation and many other cellular processes (*7*, *8*). *Xenopus* oocyte maturation includes a period termed interkinesis, during which Cdc2 becomes partially deactivated (*11*). We conjecture that the slow positive feedback loop helps prevent a transition to the off state during this critical interkinesis period.

Our study suggests that many biological systems have evolved interlinked slow and fast positive feedback loops to create reliable all-or-none switches. These dual-time switches have separately adjustable activation and deactivation times. They combine the important features of a rapid response to stimuli and a marked resistance to noise in the upstream signaling pathway.

References and Notes

1. J. E. Ferrell Jr., W. Xiong, *Chaos* **11**, 227 (2001).
2. M. Laurent, N. Kellershohn, *Trends Biochem. Sci.* **24**, 418 (1999).
3. T. S. Gardner, C. R. Cantor, J. J. Collins, *Nature* **403**, 339 (2000).
4. A. Becskei, B. Seraphin, L. Serrano, *EMBO J.* **20**, 2528 (2001).
5. F. J. Isaacs, J. Hasty, C. R. Cantor, J. J. Collins, *Proc. Natl. Acad. Sci. U.S.A.* **100**, 7714 (2003).
6. R. Wedlich-Soldner, S. C. Wai, T. Schmidt, R. Li, *J. Cell Biol.* **166**, 889 (2004).
7. M. J. Berridge, *Novartis Found. Symp.* **239**, 52 (2001).
8. R. S. Lewis, *Annu. Rev. Immunol.* **19**, 497 (2001).
9. The ordinary differential equations for the one- and two-loop positive feedback switches are

1) One loop

$$\frac{dOUT}{dt} = k_{out\_on} * A * (1 - OUT) - k_{out\_off} * OUT + k_{out\_min}$$

$$\frac{dA}{dt} = [stimulus * \frac{OUT^n}{OUT^n + ec_{50}^n} * (1 - A) - A + k_{min}] * \tau_A$$

2) Two loops

$$\frac{dOUT}{dt} = k_{out\_on} * (A + B) * (1 - OUT) - k_{out\_off} * OUT + k_{out\_min}$$

$$\frac{dA}{dt} = [stimulus * \frac{OUT^n}{OUT^n + ec_{50}^n} * (1 - A) - A + k_{min}] * \tau_A$$

$$\frac{dB}{dt} = [stimulus * \frac{OUT^n}{OUT^n + ec_{50}^n} * (1 - B) - B + k_{min}] * \tau_B$$

$k_{out\_on} = 2$, $k_{out\_off} = 0.3$, $k_{out\_min} = 0.001$, $k_{min} = 0.01$, $n = 3$, $ec_{50} = 0.35$. For a fast loop, $\tau = 0.5$. For a slow loop, $\tau = 0.008$. The equations were solved numerically with Matlab 7.0.

10. An interesting variation on this scheme can be envisioned by assuming that *A* and *B* have distinct effects on the output, and that both effects are required to activate the output. For example, *A* and *B* could phosphorylate different sites on the output protein, so that the protein is only activated when both sites are phosphorylated. The behavior of this dual-time AND switch is essentially the mirror image of the dual-time system shown in Fig. 2E: It turns on slowly, turns off rapidly, and acquires noise resistance when it has been in the off state for a period of time determined by the slow loop.
11. A. Abrieu, M. Doree, D. Fisher, *J. Cell Sci.* **114**, 257 (2001).
12. M. J. Solomon, M. Glotzer, T. H. Lee, M. Philippe, M. W. Kirschner, *Cell* **63**, 1013 (1990).
13. I. Hoffmann, P. R. Clarke, M. J. Marcote, E. Karsenti, G. Draetta, *EMBO J.* **12**, 53 (1993).
14. S. L. Harris, A. J. Levine, *Oncogene* **24**, 2899 (2005).
15. K. Levine, A. H. Tinkelenberg, F. Cross, *Prog. Cell Cycle Res.* **1**, 101 (1995).
16. A. C. Butty *et al.*, *EMBO J.* **21**, 1565 (2002).
17. R. Wedlich-Soldner, S. Altschuler, L. Wu, R. Li, *Science* **299**, 1231 (2003).
18. O. D. Weiner *et al.*, *Nat. Cell Biol.* **4**, 509 (2002).
19. M. J. Thayer *et al.*, *Cell* **58**, 241 (1989).
20. F. Cole, W. Zhang, A. Geyra, J. S. Kang, R. S. Krauss, *Dev. Cell* **7**, 843 (2004).
21. S. Kaneko *et al.*, *J. Biol. Chem.* **277**, 23230 (2002).
22. H. Singh, K. L. Medina, J. M. Pongubala, *Proc. Natl. Acad. Sci. U.S.A.* **102**, 4949 (2005).
23. K. L. Medina *et al.*, *Dev. Cell* **7**, 607 (2004).
24. H. Lodish *et al.*, *Molecular Cell Biology* (Freeman, New York, ed. 5, 2004).
25. A. R. Reynolds, C. Tischer, P. J. Verveer, O. Rocks, P. I. Bastiaens, *Nat. Cell Biol.* **5**, 447 (2003).
26. S. M. Margarit *et al.*, *Cell* **112**, 685 (2003).
27. U. S. Bhalla, P. T. Ram, R. Iyengar, *Science* **297**, 1018 (2002).
28. S. Y. Shvartsman *et al.*, *Am. J. Physiol. Cell Physiol.* **282**, C545 (2002).
29. M. Acar, A. Becskei, A. van Oudenaarden, *Nature* **435**, 228 (2005).
30. E. Beltrami, J. Jesty, *Proc. Natl. Acad. Sci. U.S.A.* **92**, 8744 (1995).
31. H. Holmsen, *Proc. Natl. Sci. Counc. Repub. China B* **15**, 147 (1991).

32. We thank R. Brandman, Y. Brandman, T. Galvez, R. S. Lewis, L. Milenkovic, D. Mochly-Rosen, M. P. Scott, P. M. Vitorino, and R. Wedlich-Soldner who provided helpful suggestions. This work was supported by an NSF predoctoral fellowship awarded to O.B., NIH grants GM46383 to J.E.F., GM057063 to R.L., and MH064801 and GM063702 to T.M.

20 April 2005; accepted 9 September 2005
10.1126/science.1113834